



Clinical Application and Multidisciplinary Assessment of Three Dimensional Printing in Double Outlet Right Ventricle With Remote Ventricular Septal Defect

World Journal for Pediatric and
Congenital Heart Surgery
2016, Vol. 7(3) 344-350
© The Author(s) 2016
Reprints and permission:
sagepub.com/journalsPermissions.nav
DOI: 10.1177/2150135116645604
pch.sagepub.com
 SAGE

Swati Garekar, MBBS, MD¹, Alpa Bharati, MD^{2,3},
Manish Chokhandre, MD¹, Shivaji Mali, DNB¹, Bhadra Trivedi, MD¹,
Vishal P. Changela, FNB¹, Narayan Solanki, MBBS²,
Sarang Gaikwad, MS, MCh¹, and Vijay Agarwal, MS, MCh, FRCS¹

Abstract

Background: Double outlet right ventricle (DORV) with two well-developed ventricles and with a remote ventricular septal defect (VSD) may present a therapeutic challenge. Echocardiographic imaging of such complex cases does not always provide all of the information required to decide on an operative approach (biventricular or univentricular) and to design an intracardiac baffle to direct left ventricular outflow through the VSD and to the aorta for biventricular repair. A three dimensional (3D) printed model of the heart based upon data derived from computed tomography (CT) or magnetic resonance imaging (MRI) may contribute to a more complete appreciation of the intracardiac anatomy. **Methods:** From April to September 2015, six consecutive patients with DORV and remote VSD underwent CT/MRI scans. Data sets from these studies were used to generate life-size 3D models using a 3D printer. We compared the assessment of 3D printed heart model findings with information obtained from echocardiography, CT, or cardiac MRI and with details of the surgeon's intraoperative direct observations when available. Quantification of the information provided by the 3D model was achieved using a unique scale that was created for the purpose of this study. The accuracy and utility of information derived preoperatively from the models were assessed. **Results:** Six data sets from six patients were analyzed. Five data sets could be successfully used to create sandstone models using 3D printing. The five patients ranged from 7 months to 11 years of age and weighed 6.7 to 26 kg. The spatial orientation of the heart in the thorax, the relationships of the great arteries and the semilunar valves, the size and location of the VSD were well appreciated in all models, as were the anticipated dimensions and orientation of a surgically planned interventricular baffle. Three of the five patients underwent successful biventricular repair. **Conclusion:** The 3D printed models scored higher than conventional imaging, with respect to most aspects of the surface spatial orientation and intracardiac anatomy. The models are a useful adjunct in pre-operative assessment of complex DORV. The unique scale helps quantify the advantages and limitations of the 3D heart models.

Keywords

congenital heart disease, double outlet right ventricle, remote ventricular septal defect, 3D printing, congenital heart disease surgery

Submitted December 11, 2015; Accepted March 08, 2016.

Introduction

The subset of double outlet right ventricle (DORV) with remote ventricular septal defect (VSD) is challenging to manage. Characteristics of this subset of DORV include a VSD that is not clearly committed to either semilunar valve (generally separated from the aortic valve by a distance of at least the dimension of the aortic annulus) or, in most cases, bilateral conus.¹ In the presence of two good-sized ventricles, the management strategy, whenever possible, is to achieve

¹ Division of Pediatric Cardiology, Fortis Child Heart Mission, Fortis Hospital, Mumbai, India

² Department of Radiology, LTMG Hospital, Sion, Mumbai, India

³ Department of Radiology, NM Medical Centre, Mumbai, India

Corresponding Author:

Swati Garekar, Division of Pediatric Cardiology, Fortis Child Heart Mission, Mulund Goregaon Link Road, Bhandup (West), Mumbai 400078, India.
Emails: swatigar@gmail.com; swati.garekar@fortishealthcare.com

Abbreviations and Acronyms

AV	atrioventricular
CT	computed tomography
3D	Three dimensional
DORV	double outlet right ventricle
MRI	magnetic resonance imaging
PA	pulmonary artery
RA	right atrium
RV	right ventricle
VSD	ventricular septal defect

biventricular repair by creating a pathway (or “tunnel”) from the left ventricle to the native (or neo) aortic valve through the VSD. This may be accompanied by surgical enlargement of the VSD. A detailed preoperative evaluation is essential for determining the feasibility of biventricular repair and for planning details of the surgical strategy.² Conventional echocardiography and real-time three dimensional (3D) echocardiography often do not provide with sufficient clarity all of the information required to plan for successful placement of an intracardiac baffle.³ At stake is biventricular repair, which, if unsuccessful, leaves the patient on the pathway to univentricular palliation.

We speculated that it would be very useful for practice and teaching purposes to create heart models using 3D printing technology in cases of DORV with potentially complex intracardiac repair. Here, we present a case series of five such cases where we printed 3D models of the patients’ hearts based on their own data from axial imaging studies. The models were assessed and rated by a radiologist, a cardiologist, and the operating surgeon.

Methods

Patients with DORV with a remote VSD and balanced, adequate-sized ventricles with normal function were selected. Standard two dimensional and color Doppler views inclusive of sweeps were obtained on Philips IE 33 (Philips Healthcare, the Netherlands). In each case, the “routability” (ie, feasibility of routing left ventricular output through the VSD to the aortic valve or neo-aortic valve) was judged to be questionable by at least one cardiologist and surgeon. All patients underwent either cardiac magnetic resonance imaging (MRI) with angiography (case 1) or contrast-enhanced computed tomography (CT; cases 2-5) imaging under deep sedation. The cardiac magnetic resonance (MR) was performed on a 3T MRI scanner (Philips Healthcare) under short deep sedation. Cine images were obtained in the standard cardiac planes followed by contrast-enhanced magnetic resonance angiography using 2 mL of gadopentetate dimeglumine injected via the left antecubital vein. Image acquisition was started once contrast reached the right ventricle (RV). Images were acquired over 12 phases using free-breathing sequence without electrocardiography (ECG) gating. Computed tomography was done on 64-detector scanner (Philips Healthcare) using bolus tracking method with 1.2 to 1.5 mL/kg of iodinated nonionic contrast material injected intravenously

(iopromide). A single postcontrast acquisition was done covering the chest without ECG gating. The average radiation exposure per study was 4.5 mSV. Using automated segmentation software, the MRI scans were selectively segmented using intensity thresholds. The automatic segmentations were reviewed followed by detailed manual segmentation so that artifacts were minimized. The relevant anatomical structures (ventricular septum, size and orientation of VSD, relationship of VSD with pulmonary artery [PA], aorta, tricuspid annulus, and ventricles) were traced. The final virtual models were converted into .stl (stereolithography) format. For case 1, parasagittal and sagittal sections of the heart (two separate models) were made. The model with parasagittal cut was found to be more informative to both the cardiologist and the cardiac surgeon. Hence, for the rest of the patients in our series, we used 3D printed models with parasagittal cuts, in addition to other sections as found necessary. The heart models were printed in sandstone (3D Systems Projet 660 pro full color printer, South Carolina) at Sahas Softech LLP (Mumbai).

The radiologist (A.B.) compared each 3D model with the CT or MR images on 11 parameters pertaining to the cardiac anatomy and planned surgery and scored the model from -2 to $+2$, with a 0 score if the 3D model gave no extra information compared to CT/MR, -2 if the model strayed from anatomy as depicted by CT/MR, or $+2$ if the 3D printed heart model gave additional information (Table 1). The cardiologist (S.G.) scored the model on the same scale, comparing it to the conventional echocardiographic clips (Table 2). The surgeon (V.A.) scored the models from 1 to 3, comparing each model to the intraoperative findings for each of the three cases that underwent biventricular repair. A score of 1 meant least accurate, whereas 3 was most accurate (Table 3).

Results

Patients

Six consecutive patients with DORV, remote VSD, and questionable intracardiac routability underwent MRI (1 patient) or CT (5 patients) scans between April and September 2015. For one patient, the CT data were found to be deficient and a model could not be made. The demographics and detailed anatomy of the remaining five patients are detailed in Table 4. In brief, the great arteries were abnormally related in all cases. Cases 2 and 5 had D-malposition. Case 1 had side-by-side great arteries with the aorta to the right. Cases 3 and 4 had anteroposterior relationship of the great arteries. The VSD was large and in the inlet region in all cases. The tricuspid valve leaflets were normal in all cases. Two of the five cases (cases 3 and 5) had a few tricuspid valve leaflet chordae attached to the crest of the ventricular septum. Three of the five cases (cases 2-4) had important valvar pulmonary stenosis inclusive of annular hypoplasia. Case 1 had mild valvar and subvalvar pulmonary stenosis, and case 5 had severe valvar and subvalvar stenosis. Case 3 had a major coronary artery on the epicardium of the RV outflow tract.

Table 1. Radiologist's Scale.^a

Parameter	Case 1	Case 2	Case 3	Case 4	Case 5
Spatial orientation	0	0	0	0	0
Relationship of aorta and main pulmonary artery	+2	+2	+2	+2	+2
Relationship of aortic and pulmonary valve	0	0	0	0	0
VSD size	-1	+1	+1	+2	+1
VSD position	+2	+2	+2	+2	+2
Predicted baffle length	+2	+2	+2	+1	+2
Tricuspid valve chordae	-2	+2	+2	-1	+2
Aortic valve	+1	+1	+1	+1	+1
RVOT	+2	NA	0	NA	NA
Predicted RVOT obstruction by baffle	+2	NA	+1	NA	NA
Predicted RV encroachment by baffle	+2	+2	+2	+2	+2
Decision-making	+2	+2	+2	+2	+2

Abbreviations: CT, computed tomography; 3D, 3-dimensional; MRI, magnetic resonance imaging; NA, not available; RV, right ventricle; RVOT, right ventricular outflow tract; VSD, ventricular septal defect.

^aScale: -2 to +2. Scale as assessed by radiologist. The radiologist compared the 3D model with CT/MRI and scored the model from -2 to +2, with score 0 if the 3D model gave no extra information compared to CT/MRI, -2 if the model strayed from anatomy as depicted by CT/MRI, or +2 if the 3D printed heart model gave additional information.

Table 2. Cardiologist's Scale.^a

Parameter	Case 1	Case 2	Case 3	Case 4	Case 5
Spatial orientation	+2	+2	+2	+2	+2
Relationship of aorta and main pulmonary artery	+2	+2	+2	NA	+2
Relationship of aortic and pulmonary valve	0	0	0	0	0
VSD size	-2	-2	0	-1	-2
VSD position	+1	+1	+2	+1	+1
Predicted baffle length	+2	+2	+2	+2	+2
Tricuspid valve chordae	-2	-2	+1	-2	-2
Aortic valve	-2	-2	-2	-2	-2
RVOT	+2	NA	+2	NA	NA
Predicted RVOT obstruction by baffle	+2	NA	+2	NA	NA
Predicted RV encroachment by baffle	-1	-1	+2	+2	+1
Decision-making	+2	+2	+1	+2	+1

Abbreviations: 3D, 3-dimensional; NA, not available; RV, right ventricle; RVOT, right ventricular outflow tract; VSD, ventricular septal defect.

^aScale: -2 to +2. Scale as assessed by cardiologist. The cardiologist compared the 3D model with conventional echocardiography and scored the model from -2 to +2, with score 0 if the 3D model gave no extra information compared to echocardiography, -2 if the model strayed from anatomy as depicted by echocardiography, or +2 if the 3D printed heart model gave additional information.

Table 3. Surgeons Scale.^a

Parameter	Case 1	Case 2	Case 4
Spatial orientation	3	3	3
Great artery relationship	3	3	3
VSD size	3	2	3
VSD position	3	2	3
Predicted baffle length	3	3	3
Tricuspid valve chordae	1	1	1
Aortic annulus	3	3	3
RVOT	3	NA	NA
Predicted RVOT obstruction by baffle	3	NA	NA
Predicted RV encroachment by baffle	3	3	3
Decision-making	3	3	3

Abbreviations: 3D, 3-dimensional; RV, right ventricle; RVOT, right ventricular outflow tract; VSD, ventricular septal defect.

^aScale: 1 to 3 (least accurate/precise/reliable to accurate/precise/reliable).

Comparison of various parameters on 3D heart model versus intraoperative findings by the cardiac surgeon.

Three Dimensional Printed Heart Models

The macroscopic size and structure of the models resembled that of an actual heart. Upon closer inspection, a layered structure could be seen as a result of the systematic layering of sandstone by the 3D printer. The descending aorta and a small length of the superior vena cava and inferior vena cava were deliberately retained to serve as landmarks that helped anatomic and spatial orientation of the model (Figures 1 and 2). The anatomy was studied from the surgical perspective by printing models with removal of the anterior wall of the RV and part of the right atrium (RA). The virtual heart model was studied on the Digital Imaging and Communications in Medicine (DICOM) file, and relevant (paraseptal) sections were made. The DICOM file was then converted into .stl for printing of the "sectioned" models. An individualized approach was carried out in "slicing" the model to obtain the most relevant anatomy from the surgical viewpoint. Each model had at least

Table 4. Patient Demographics, Diagnosis, and Surgical Outcome.

Case No.	Age/Weight (kg)	Echocardiography Diagnosis	Surgery Options	Surgery Performed
1	7 months/6.8	DORV with large inlet VSD with side-by-side great arteries (aorta right); mild PS	PA band or LV to aorta baffle	Biventricular repair by LV to aorta baffle
2	6 years/15.6	DORV, large inlet VSD, D-malposed great arteries, severe PS with annular hypoplasia	BD Glenn or LV to aorta baffle and RV to PA conduit	Biventricular repair by LV to aorta baffle and RV to PA conduit
3	2 years/9 ^a	DORV, large inlet VSD, anteroposterior great arteries, severe PS with annular hypoplasia	BD Glenn or LV to aorta baffle with RV to PA conduit	BD Glenn shunt with LPA plasty
4	11 years/26	CC-TGA, DORV, large inlet VSD, severe PS with annular hypoplasia (status post bidirectional Glenn shunt)	Fontan or Senning with LV to aorta baffle with RV to PA conduit	One-and-a-half ventricle repair with hemi-Mustard
5	3.5 years/8	Situs inversus, CC-TGA, DORV, large inlet VSD, severe PS with annular hypoplasia	BD Glenn or Senning with LV to aorta baffle with RV to PA conduit	Awaiting surgery

Abbreviations: BD, bidirectional; CC-TGA, congenitally corrected transposition of great arteries; DORV, double outlet right ventricle; LPA, left pulmonary artery; LV, left ventricle; PA, pulmonary artery; PS, pulmonary stenosis; RV, right ventricle; RVOT, right ventricular outflow tract; VSD, ventricular septal defect.

^aDecision to perform bidirectional Glenn shunt was taken as there was associated diaphragm eventration and a very posteriorly placed right atrium, a major coronary crossing the RVOT and severe LPA ostial stenosis.

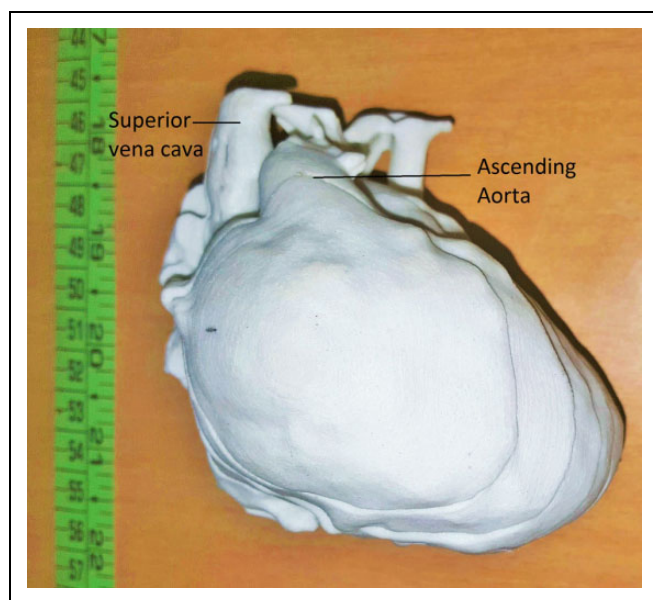


Figure 1. Anterior surface view of the life-size 3-dimensional (3D) heart model of case 1, a case of double outlet right ventricle with side-by-side great arteries and large inlet ventricular septal defect (VSD).

four sections made (range: 4-8). In all the cases, a large portion of the ventricular septum was seen en face, and the VSD was well defined as parasagittal sections were made. The aortic and pulmonary annuli were also well defined, and hence their relationship to each other, to the ventricular mass, and to the VSD were well appreciated in all cases. This made it possible to anticipate the potential location and dimensions of the baffle (from the VSD to the aorta). All models defined the atrioventricular (AV) valve annular ring. The MRI-based heart model did not feature any AV valve chordae. The remaining CT-based heart models showed

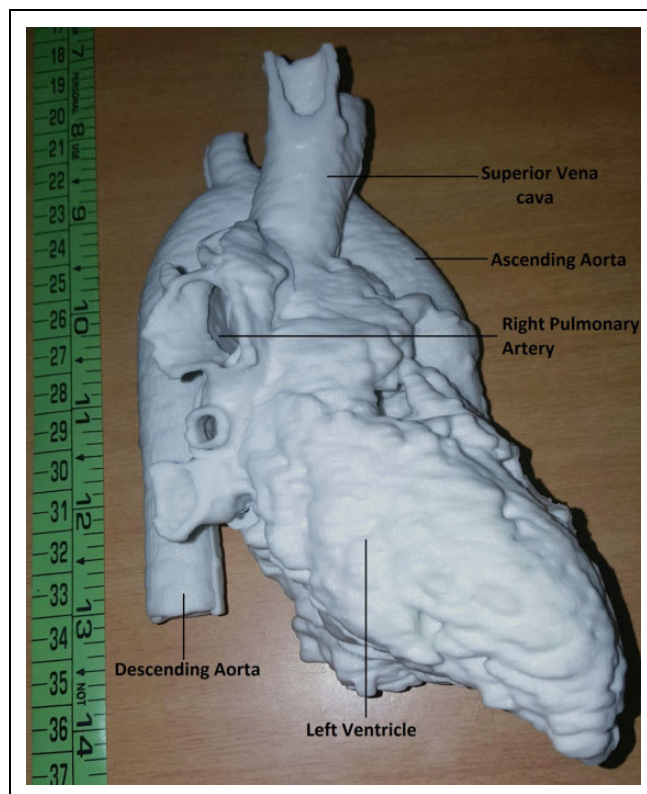


Figure 2. Right lateral surface view of the life-size three dimensional heart model of case 4, a case of congenitally corrected transposition of the great arteries with a double outlet right ventricle, L-malposed great arteries, large inlet ventricular septal defect, status post main pulmonary artery ligation, and bidirectional Glenn anastomosis.

only the most prominent chordae of the AV valves. The radiologist felt that accurate information regarding the spatial orientation and the relationships of the aortic and pulmonary valves was obtained from the CT/MRI images, and hence, all models were

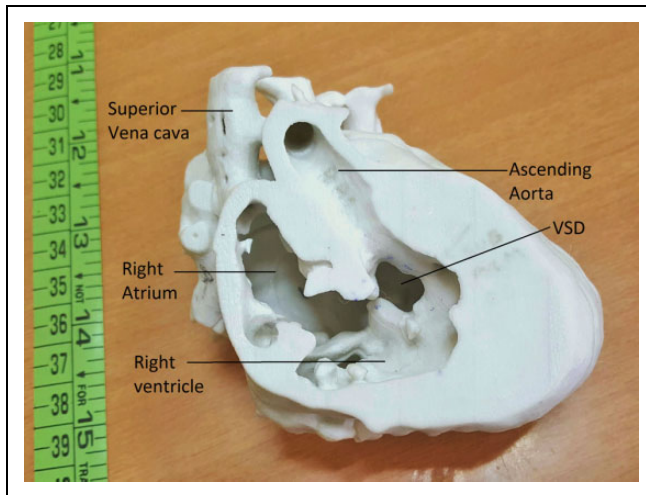


Figure 3. A paraseptal slice of the heart model of case 1 showing the surgical view: inlet ventricular septal defect, intervening muscle and aorta as seen from the right ventricular aspect.

scored 0 in that aspect by her (Table 1). From the radiologist's viewpoint, the models provided a significant advantage over CT/MRI in displaying great artery relationship, VSD position, and all aspects of the baffle (scores of +2 in Table 1).

Overall, the models showed significant advantage (score of +1 or more) over echocardiography when assessed for spatial orientation of the heart, great artery relationship to each other (main PA and ascending aorta), VSD location, baffle lie, estimated baffle length, and impact of the baffle on the RV outflow tract or RV cavity (Table 2). The VSD size was adjudged to be more accurate on echocardiography than on the models due to non-ECG gating. The estimated baffle length was easier to predict on the models.

The intraoperative comparison (cases 1, 2, and 4) by the cardiovascular surgeon revealed agreement (score of 3) with the model in most aspects, except for tricuspid valve chordal anatomy (Table 3). There was disparity in the VSD size, as expected. Case 1 ultimately required VSD enlargement. The intraoperative view through the tricuspid valve was similar to that seen in the paraseptal slice of the model (Figure 3).

The surface spatial orientation provided by the model was especially useful in patients with coexistent heterotaxy. The model helped plan the precise site for right ventriculotomy (and conduit placement) in cases 2 and 4. The location and lie of the conduit could be planned, as the relationships and orientation of the main and branch pulmonary arteries were well delineated on the models. In case 4, the hemi-Mustard procedure was also visualized preoperatively using the model. The tricuspid annulus was well defined, though the leaflets and the chordae were not generally visible. However, in one case (case 3), we could print chordae of the tricuspid valve as there were extensive thick chordae visible. Overall, the models were rated negative for tricuspid valve anatomy. The anatomy of the semilunar valves was also assessed to be better seen on echocardiography. However, the annulus of the aortic valve was clearly delineated

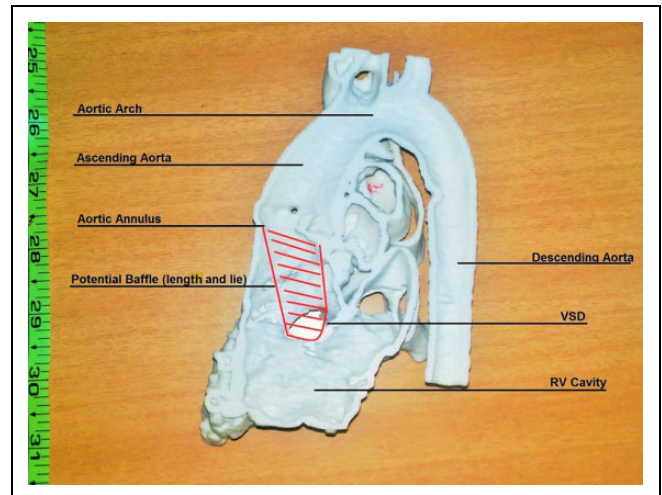


Figure 4. Position of proposed intraventricular baffle from the ventricular septal defect to the aortic valve is shown (lines drawn in).

on all the models and hence served the purpose of estimating the length of the intraventricular baffle (Figure 4).

The models significantly helped in decision-making. The models clearly were not the only modality used for decision-making. Rather they complemented the existing modalities. The success of biventricular repair is based on multiple factors including accurate assessment of the type, size, and location of the VSD, great artery relationship, conal anatomy, AV valve chordal anatomy, and coronary artery anatomy. The 3D printed heart models shed more light on some of these features. Cases 1 and 4 were likely to have undergone PA banding and Fontan completion, respectively, based on the impressions derived from conventional imaging studies. Their 3D printed heart models played a significant role in the decision-making that led to successful biventricular and one-and-a-half ventricular repair, respectively. In case 2, the 3D model gave the surgeon more information and confidence preoperatively to plan the operation and communicate with the parents.

The models were also seen by pediatric cardiac anesthesiologists, intensivists, and trainees in pediatric cardiology. The complex intracardiac anatomy was easily understood using the models. They seemed to be a good tool for teaching.

Four of the five patients underwent cardiac surgery, of which three (cases 1, 2, and 4) underwent successful biventricular repair (case 4 had a one-and-a-half ventricle repair as his preexisting Glenn shunt was left in place). No attempt was made to compare intraoperative times (bypass times or aortic cross-clamp times) of these patients versus those without models. One patient (case 3) had associated diaphragm eventration and a very posteriorly placed RA, a major coronary crossing the right ventricular outflow tract and severe proximal left PA stenosis. A decision was taken to proceed with a Glenn palliation. Intracardiac inspection was not performed. Case 5 is awaiting surgery. Patients who underwent complete intracardiac repair showed satisfactory clinical and echocardiographic progress on follow-up evaluation (range: 1-6 months).

Discussion

Double outlet right ventricle with remote VSD still represents a significant therapeutic challenge, despite multiple reports of encouraging results of achieving biventricular repair.¹ The critically important aspect of “routability of the left ventricle to the aorta” (ie, the feasibility of implanting a baffle to create an intraventricular tunnel from the VSD to the aorta) is challenging to assess completely on the basis of information obtained from conventional echocardiography. With the advent of real-time 3D echocardiography, it has become easier to “visualize” the planned location and dimensions of the potential baffle.³ However, a communication gap may still exist between the cardiologist and the surgeon while evaluating the 3D echocardiogram. Recently, virtual 3D heart models generated from cardiac MR data sets have been used to delineate the intracardiac anatomy in complex DORV.⁴ However, the high-resolution MR sequences required for this are not universally available. Three dimensional printed models may help to bridge the communication gap between the radiologist and the surgeon, which may otherwise continue to be an obstacle to complete understanding.

Three dimensional printing, or additive manufacturing, was first described in the early 1980s by Charles Hull who called it “stereolithography.” Data are stored in a .stl format that allows interpretation of the data in a computer-aided design (CAD) file that can be read by a 3D printer. Along with the shape, the instructions in the .stl file may also include information such as the color, texture, and thickness of the object to be printed.^{5,6} Numerous applications of 3D printing for heart disease are well described.⁷ Our case series demonstrate that life-size 3D printed heart models can help in presurgical planning. Relative to the original imaging modalities, the models provided additional information for most parameters on which they were scored. The scores of the surgeon for the three patients who underwent biventricular repair also reflect a high level of satisfaction with the anatomy displayed by the model. The models could be independently studied by the surgical team, and thus, a difference of opinion about terminology and subjective analysis of the intracardiac anatomy was mitigated to a large extent. Overall, the confidence of the team with regard to predicting suitability for biventricular repair in the operation suite was enhanced by the 3D printed model.

Echocardiography provides limited information with respect to assessment of the surface anatomy of the heart. The 3D printed heart model shows this in an indisputable manner. The spatial orientation of the heart that clearly showed the spatial relationships of the ventricles, atria, and vessels helped presurgical planning, over and above the advantage offered in delineating the intracardiac anatomy. This is significant as the presence of heterotaxy and malrotated hearts can influence the decision to proceed with Senning/Mustard types of atrial baffle procedures in complex DORV.

Echocardiographic sweeps (acquisition of the anteroposterior or medial–lateral anatomy of the heart as a continuous recording from an imaging window) form an essential part of

imaging of complex intracardiac anatomy and help deduce 3D spatial relationships. However, surgical understanding of the sweeps may be challenging. The 3D printed heart models convey the information in a straightforward manner and with elimination of bias introduced by terminology. The paraseptal view of the VSD and its relationship to the aorta on the 3D printed heart model was similar to the surgical view.

In case 4, the immediate preoperative echocardiographic windows were limited and the imaging quality was poor. However, the 3D printed model clearly demonstrated the intracardiac and surface anatomy.

Our 3D printed models appear to be useful in presurgical planning, despite the opaque and nonelastic nature of the material used. This use of sandstone “printing” material resulted in significant cost savings (a potentially important benefit to the patient) compared to the use of transparent or elastic material, which is available and could certainly be used in specific instances where it may be perceived to be advantageous.

Limitation of the Scale Devised to Quantify Utility of Three Dimensional Models

There is a potential for bias as the surgeon scored the model after having seen the echocardiographic and CT/MRI images. A positive rating (of 3, on a scale of 0-3) by the surgeon may have been influenced by greater clarity afforded by the model compared to echocardiography/CT/MRI. An example of this is in the estimation of the potential baffle length, rated as a 3 in each of the operated cases. Even though the model-based estimate may not have been precisely accurate in comparison to intraoperative findings, the surgeon may have rated it high as the information from echo/CT was less useful or the estimate based on those images was far from accurate.

It has to be emphasized that the positive scores given by the radiologist and the cardiologist reflect their assessment of an advantage relative to the information available from CT/MRI/echocardiography without the printed model. High scores do not imply that there is complete agreement with intraoperative findings.

The ideal scale would be one that can be scored by a single person who can reliably interpret CT/MRI/echocardiography and then correlate with intraoperative findings. Multiple physicians could utilize the scale to eliminate reporting bias.

Limitations of the 3D Printed Models

The MRI or CT was not gated to ECG or respiration, implying that the model was a composite. The dimensions of the VSD displayed in the model could thus be inaccurate. The tricuspid valve leaflets and chordae were not well represented and reliably delineated in our 3D heart models.

Radiation exposure is a concern with CT imaging. However, the amount of radiation exposure in our CT imaging protocol was an average of 4.5 mSv. This is approximately equal to four

years' worth of background natural radiation with a very low to low additional risk of occurrence of cancer in the lifetime.

Our choice of sandstone material meant that the model did not have a "real" feel. The real-time change in dimension and volume with systole and diastole has to be kept in mind when interpreting the rigid heart model. Models made by 3D printing may have the same softness and resistance as real cardiac tissues, though this depends somewhat on the choice of material. With respect to printing of vascular structures, the models do not accurately represent wall fragility and alterations due to endovascular flow of a real arterial system. These limitations and others should be considered during testing. Our models were opaque; hence, we sliced them for a fuller appreciation of the intracardiac anatomy. The slicing has to be tailored to the individual patient anatomy. At this point, we are still in the process of forming protocols for slicing.

The ideal 3D model. The ideal 3D printed model might be a diastolic-phase printed model of the heart with no distortion due to respiration. The intracardiac anatomy would be preserved, inclusive of small AV valve chordae. The basis for the model would be a noncontrast high (submillimeter) spatial resolution volumetric interpolated breath hold examination sequence on MRI. The material for the print would mimic the texture of the myocardium. Multiple printing colors that can differentiate atria from ventricles from vessels would be available, further improving the ease of understanding. Computer simulation of the repaired heart's anatomy with the baffle in place followed by its 3D printed model would represent an additional step toward completion of the battery of investigations, leaving actual execution of the surgical plan as the final step. Computational flow dynamics following baffle placement could also be studied on the virtual model.

Conclusion

Three dimensional printed heart models are useful in presurgical planning in complex DORV in our case series. Their availability facilitates multidisciplinary team involvement and may help to mitigate communication gaps between the cardiologist/radiologist and the surgeon. The preoperative confidence level

in contemplating, choosing, and carrying out a biventricular repair was enhanced by the opportunity to study life-size 3D models derived from patient-specific data in three of our patients. The advantages and limitations of 3D printed heart models will become more apparent with additional experience and refinements of this modality.

Declaration of Conflicting Interests

The author(s) declared no potential conflicts of interest with respect to the research, authorship, and/or publication of this article.

Funding

The author(s) received no financial support for the research, authorship, and/or publication of this article.

References

1. Lacour-Gayet F. Biventricular repair of double outlet right ventricle with noncommitted ventricular septal defect. *Semin Thorac Cardiovasc Surg Pediatr Card Surg Annu.* 2002;5: 163-172.
2. Li S, Ma K, Hu S, et al. Biventricular repair for double outlet right ventricle with non-committed ventricular septal defect. *Eur J Cardiothorac Surg.* 2015;48(4): 580-587; discussion 587.
3. Pushparajah K, Barlow A, Tran VH, et al. A systematic three-dimensional echocardiographic approach to assist surgical planning in double outlet right ventricle. *Echocardiography.* 2013; 30(2): 234-238.
4. Farooqi KM, Uppu SC, Nguyen K, et al. Application of virtual three-dimensional models for simultaneous visualization of intracardiac anatomic relationships in double outlet right ventricle. *Pediatr Cardiol.* 2016;37(1): 90-98.
5. Schubert C, van Langeveld MC, Donoso LA. Innovations in 3D printing: a 3D overview from optics to organs. *Br J Ophthalmol.* 2014;98(2): 159-161.
6. Gross BC, Erkal JL, Lockwood SY, Chen C, Spence DM. Evaluation of 3D printing and its potential impact on biotechnology and the chemical sciences. *Anal Chem.* 2014;86(7): 3240-3253.
7. Itagaki MW. Using 3D printed models for planning and guidance during endovascular intervention: a technical advance. *Diagn Interv Radiol.* 2015;21(4): 338-341.